Numerical modelling of the microwave heating behaviour of lunar regolith

Journal Item

Numerical modelling of the microwave heating behaviour of lunar regolith

Sungwoo Lim† and Mahesh Anand

School of Physical Sciences, Faculty of Science, Technology, Engineering and Mathematics, The Open University, Walton Hall, Milton Keynes, MK7 6AA, UK

† Corresponding author: sungwoo.lim@open.ac.uk

Abstract

The field of *In Situ* Resource Utilisation (ISRU) is expanding rapidly with a particular focus on developing ISRU technologies and applications to support a longer-term surface exploration of the Moon. In this respect, microwave sintering is proposed to be one of the potential fabrication methods for developing a 3D printing technique for construction processes on the Moon. Thus, understanding the behaviour of lunar regolith, available at different locations on the Moon (e.g. mare versus highlands regions), under microwave heating is crucial for developing an optimal method for microwave sintering. As the availability of real lunar regolith on Earth is highly limited, developing an appropriate numerical model of microwave heating behaviour of lunar regolith is urgently required. In this paper, three representative lunar regolith samples (selected from the database of Apollo sample collections) with pre-defined material properties have been simulated under seven input powers and three specimen sizes. This paper discusses the outcomes of these simulations and the potential contribution of the model for developing a desired 3D printing technique utilising microwave sintering of lunar regolith.

Keywords

ISRU, Numerical modelling, Microwave heating, Lunar regolith, Extra-terrestrial Construction, COMSOL

1. Introduction

As described in Lim et al. (2017), 3D Printing is considered as one of the possible techniques for realising extra-terrestrial construction processes on the Moon and Mars. Recent initiatives including NASA and ESA's lunar *In-Situ* Resource Utilization (ISRU) demonstration activities as part of the Deep Space Gateway concept are encouraging researchers and practitioners for developing an appropriate fabrication method for supporting lunar construction processes.

Microwave sintering is proposed as one of the potential fabrication methods for 3D printing technique, which could be utilised for extra-terrestrial construction processes. For example, the thermal conductivity of the lunar regolith is very low depending on the depth (Hayne et al. 2017). Therefore, the lunar regolith could act as an excellent thermal insulator. This property, however, also means that direct heating of the regolith using a laser or solar energy would not be an effective method for heating the subsurface regolith. However, microwave energy can penetrate deeper into the lunar regolith and heat the subsurface regolith with radiant heat efficiently (Ethridge and Kaukler 2012). More detailed background and rationale of developing a microwave sintering-based 3D printing technique as part of an extra-terrestrial construction process have been given in Lim et al. (2017). Our previous experiments (Levin Prabhu et al. 2018), which involved heating of two lunar simulants, JSC-1A (35 g) and NU-LHT-3M (35 g), using a domestic microwave with 1 kW of input power, demonstrated that JSC-1A was sintered/melted in 480 seconds while NU-LHT-3M did not sinter even though 10% ilmenite was added as a susceptor and heating was continued up to 1,200 seconds. Taylor and Meek (2004, 2005) and Taylor et al. (2005) hypothesised that lunar regolith would couple well with microwave energy and that it would take much less time to heat real lunar samples compared to the lunar simulants due to the presence of nano-phase iron (Taylor and Meek 2005), FeO, or irregularly shaped particles (Taylor and Meek 2005, Taylor and Liu 2010, Barmatz et al. 2013).

A computer-based numerical modelling is a useful way to optimise a microwave system design and conduct a realistic process simulation for given material properties, dimension and mass/volume of a sample and the ideal conditions of the system (National_Research_Council, 1994). In addition, it could also verify Taylor and Meek's hypothesis, prior to visiting the Moon for sampling resources . Although a few previous studies (Ethridge and Kaukler 2011, Ethridge and Kaukler 2012, Allan et al. 2013) discussed the numerical modelling of microwave heating behaviour of lunar simulants, no such work has been done for the real lunar regolith. As the availability of real lunar regolith is highly limited, we have set about establishing a fully defined numerical model of microwave heating behaviour of lunar regolith by combining existing information regarding the material properties of lunar regolith as a complementary solution for our future lab experiments using real lunar samples.

2. Aims & objectives

The primary purpose of establishing a fully defined numerical model is to understand better whether raw lunar regolith couples well with microwave energy under specific input power to be a potential lunar construction material. The objectives of this work are to (i) find appropriate parameters/settings including the material properties of lunar regolith for a simulation in COMSOL Multiphysics software; (ii) compare the microwave heating behaviour of different lunar regolith, by location (i.e. highlands, mare with high-titanium and mare with low-titanium composition), input power and mass of specimen; and (iii) identify an optimal setting – input power and heating time, etc. – for extracting volatiles and sintering material that can be used for ISRU derived lunar missions, i.e. production of water, oxygen and construction process.

3. Experimental settings for the simulation of the numerical model

The Space Instrumentation Group at The Open University has recently started investigating microwave sintering of lunar regolith/simulant as a potential fabrication method of 3D printing on the Moon to build lunar habitats. As part of this initiative, we are currently manufacturing an industrial bespoke microwave heating equipment. As complementary research, we are developing numerical models of microwave heating behaviour of lunar regolith using the bespoke microwave cavity and the material properties of lunar regolith as a function of temperature. Simulation of the model has been conducted using a COMSOL Multiphysics software (version 5.3a) with a Radio Frequency (RF), Heat Transfer and Design modules.

3.1 Bespoke microwave heating equipment

The industrial bespoke microwave heating equipment has been designed to overcome the limitation of a domestic microwave, which is not capable of (i) withstanding high temperatures, e.g. the melting temperature of lunar regolith; (ii) providing a vacuumed cavity condition; (iii) controlling the input power; and (iv) monitoring and recording the temperature changes of a specimen as a function of time. In addition, unlike a domestic microwave oven, the bespoke microwave works in a single-mode where one resonant mode is excited, allowing higher energy efficiency than a domestic microwave oven (Hoogenboom et al. 2009). Figure 1 illustrates a design of the equipment that includes two pyrometer ports, one naked-eye viewer window, and a cylindrical cavity with a flange for a vacuum pump. The cavity can also be connected to a mass spectrometer, permitting extraction and analysis of volatiles while a specimen is being heated. Volatiles in regolith can be extracted by heating the regolith between 300 and 900 °C (Anand et al. 2012, Ethridge and Kaukler 2012), and most of the H_2 can also be extracted up to 700 °C (Crawford 2015), which are needed for producing water using oxygen extracted from lunar regolith. Thus, the equipment could also be used for measuring the types and volume of extracted volatiles which could be used for propellant and life support (e.g. water and oxygen). It is expected that the new equipment would allow to (i) maximise microwave energy in a single hotspot; (ii) measure the surface temperature and phase change of a specimen under near lunar atmospheric condition more accurately; and (iii) heat a specimen of lunar regolith/simulant rapidly to be sintered/melted. In this experiment, only the cavity and the input port of the equipment are modelled in COMSOL to simplify the simulation experiment. This first version of the equipment does not support multiple frequencies, which requires a redesign of cavity dimension; however, this feature is planned to be added in a future upgrade.

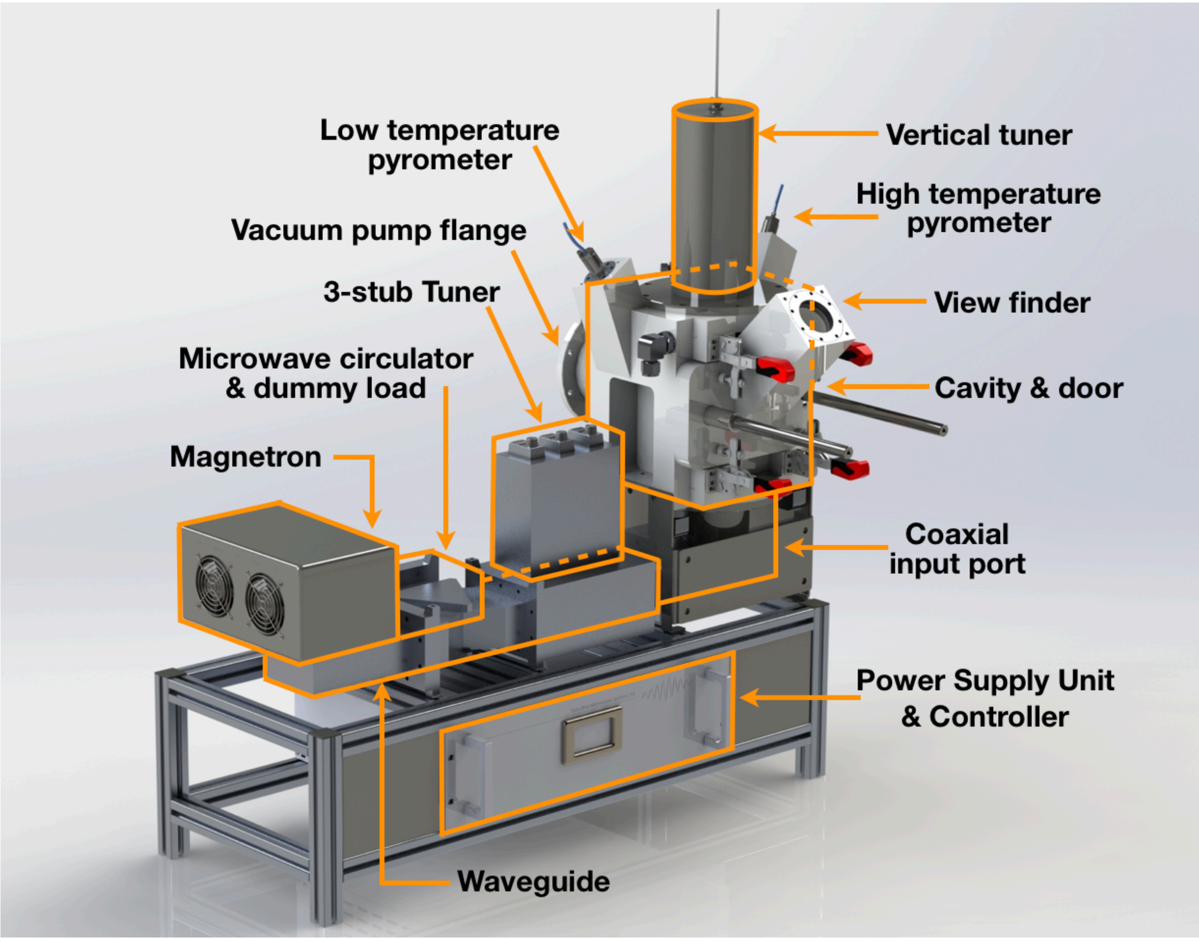

Figure 1: The bespoke microwave heating equipment with a vacuum cavity. The dimension of the equipment is 860 (Length) x 340 (Depth) x 1,037 (Height) mm.

3.2 Material properties of lunar regolith

The materials used in this experiment are based on the three categorisations from Schreiner et al. (2016), which are highlands regolith (highlands, TiO_2 0.5 wt%, FeO 6.2 wt%), mare high-titanium regolith (mare High-Ti, TiO_2 8.5 wt%, FeO 16.6 wt%) and mare low-titanium regolith (mare Low-Ti, TiO_2 2.9 wt%, FeO 17 wt%). All material properties should be defined as a function of temperature to simulate proper microwave heating behaviour. Although existing literature are scattered across conference abstracts, technical reports and peer-reviewed journals, the work by Schreiner et al. (2016) covers most of the material properties of lunar regolith needed for developing a numerical model of microwave heating behaviour of lunar regolith and a simulation. Thus, we have adopted most of the model of Schreiner et al. (2016) in our experiment. Note that the material properties discussed below are required for simulating the designed numerical model in COMSOL.

Density (g/cm³)

Researchers measured a solid density of lunar regolith as 1.5 ~ 1.9 g/cm^3 (Mitchell et al. 1974, Heiken et al. 1991, McKay et al. 1991). In our previous experiment, we fabricated compressed pellets, the density of which was 2.07 g/cm^3. As we are also planning to use a compressed pellet with the bespoke microwave heating equipment, we have defined the solid density of lunar regolith for this simulation as 2.07 g/cm^3. For a molten density of lunar regolith, we used the density model equation below proposed by Schreiner et al. (2016), which manipulates the Stebbins' equation (1984) algebraically

$$\rho = \frac{r_1}{r_2 + r_3(T - 1873)}$$

where ρ is the density (kg/m^3), T is the temperature (K), and r_i are regression coefficients, which can be found in (Schreiner et al. 2016). In this experiment, we have defined the density of lunar regolith starting with a compressed pellet density of 2.07 g/cm^3 until the melting temperature *MeT* (1,500 K), and adapted Schreiner et al.'s equation until the density reduces to 1.66 g/cm^3, which is the average bulk density on the Moon at a depth of between 0 ~ 60 cm (Mitchell et al. 1974). The adapted plot is displayed to 2,000K (see Figure 2).

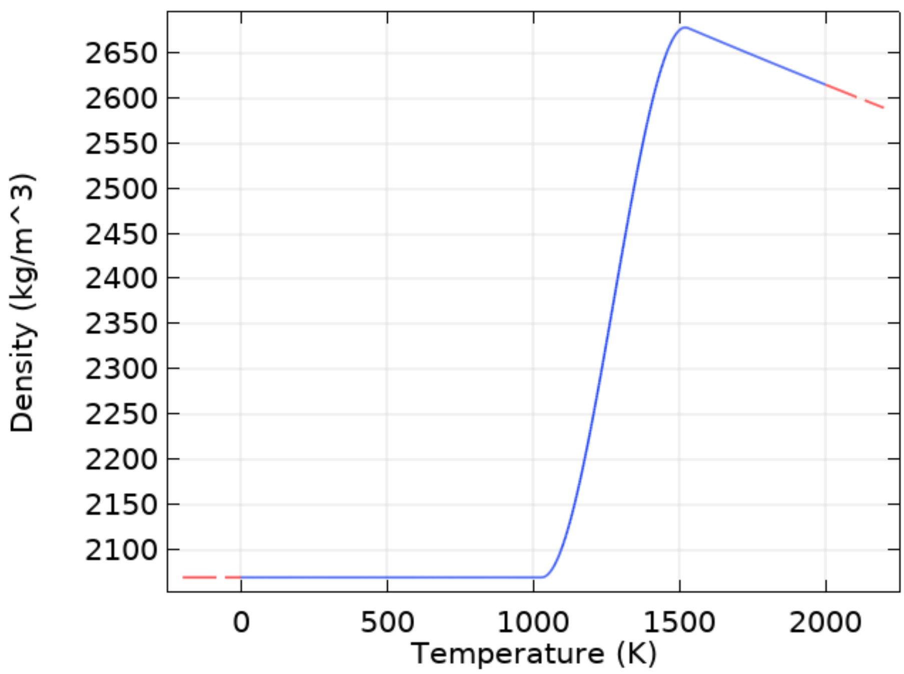

Figure 2: Material properties – Density of highlands regolith as a function of temperature.

*Heat capacity (J/(kg*K))*

Previous researchers (Marcus et al. 1973) found that the melting temperature of lunar regolith varied between 1,373 K and 1,653 K (~1,100 to 1,380 °C) although there is no report on specific melting temperatures for highlands and mare regolith. Thus, in this experiment, we have defined an initial melting temperature as 1,373 K (1,099.85 °C) and completely molten temperature as 1,653K (1,379.85 °C) to be used for three regolith types. Reiss (2018) pointed out that the heat capacity model from Schreiner et al. (2016) is most appropriate as it combines three temperature categories: (i) below 350 K (76.85 °C) (Hemingway et al. 1973), (ii) above 250 K and below the melting temperature - 1,500 K (Stebbins et al. 1984), and (iii) above the melting temperature (Stebbins et al. 1984). Thus, we have adopted Schreiner et al. (2016)'s approach (Figure 3).

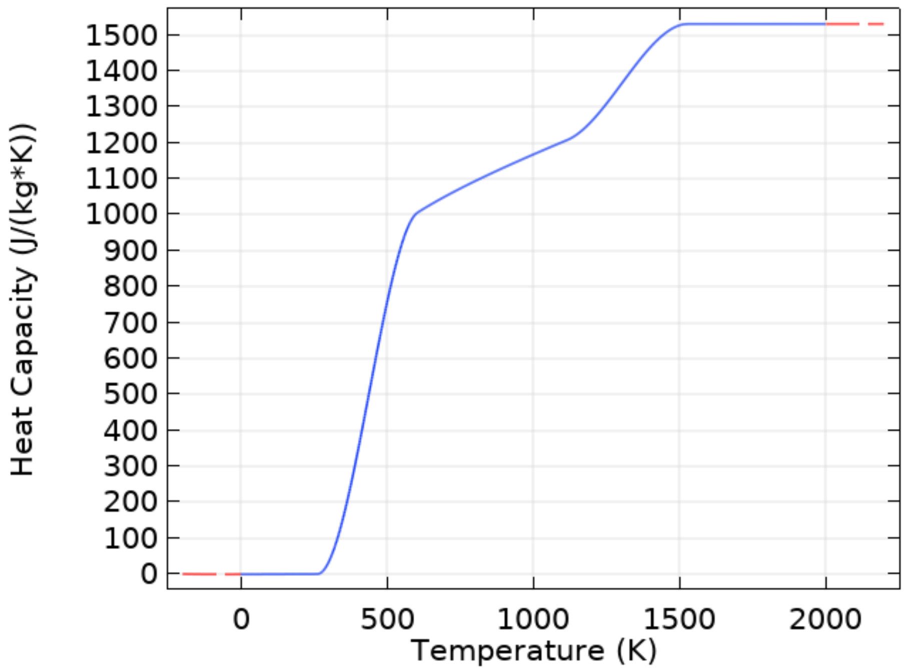

Figure 3: Material properties – Heat Capacity of highlands regolith as a function of temperature.

*Thermal conductivity (W/m*K)*

As for the density of lunar regolith, researchers also measured the thermal conductivity of lunar regolith via two stages: as solid (Langseth et al. 1972, Cremers 2012) and as in molten state (Kang and Morita 2006) without distinguishing them by location. Because of the gaps between the two data, Schreiner et al. (2016) suggested a continuous model fit as below

$$k = \frac{0.01257\left(T^{'}\right) + 0.0172}{(T^{'})^{2}\text{-}2.874(T^{'}) + 2.085}$$

where *K* is thermal conductivity (W/m*K), $T^{'}$ is the temperature (K) normalised by a mean 691.7 and standard deviation 564.3. This model fit, however, does not show a realistic thermal behaviour because the conductivity is decreased after the melting temperature. As was explained by Colozza (1991), the thermal conductivity of lunar regolith increases as the temperature increases until it reaches the initial melting point (1,373K) then decreases linearly with temperature until it reaches the completely molten temperature (1,653K). Thus, in this experiment, we have adapted the thermal conductivity model of Colozza (1991), which extended Murase and McBirney (1970)'s equation above the melting temperature of lunar regolith. Because Colozza did not provide the equation of the extended part, we have extracted the data from Colozza's plot (Figure 2 in (Colozza 1991)) and interpolated them in COMSOL to create a similar curve (see Figure 4).

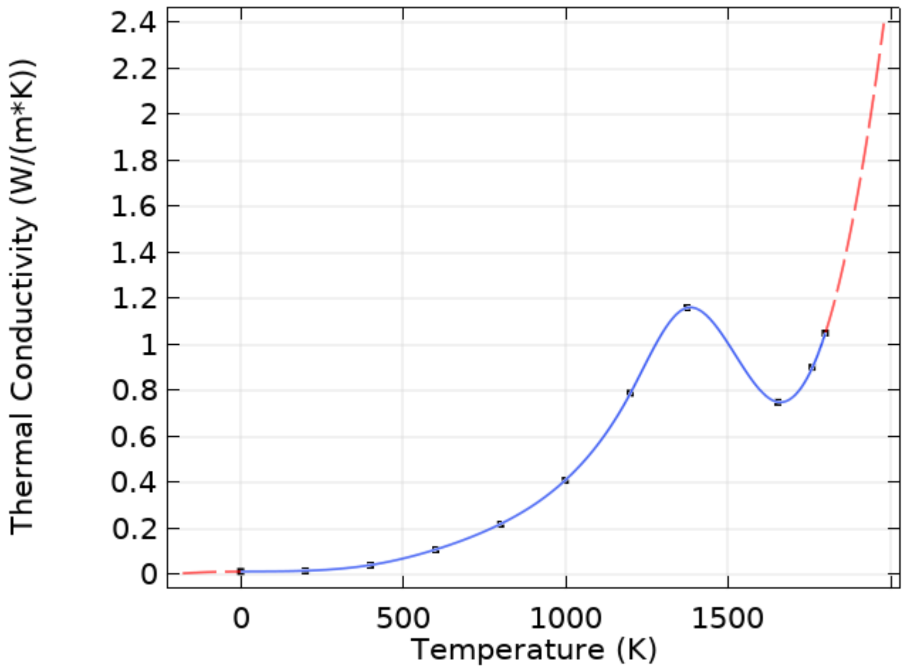

Figure 4: Material properties – Thermal Conductivity of highlands regolith as a function of temperature.

The above data can also be interpolated with a cubic spline interpolation method applying the equations with cases below.

$$f(x) = \begin{cases} 4.0486 \cdot 10^{-10} \cdot x^3 + 4.6278 \cdot 10^{-61} \cdot x^2 + 1.5295 \cdot 10^{-6} \cdot x + 1.2810 \cdot 10^{-2}, & \text{if } x \in [0,200], \\ 6.3429 \cdot 10^{-10} \cdot x^3 - 1.3766 \cdot 10^{-7} \cdot x^2 + 2.9061 \cdot 10^{-5} \cdot x + 1.0975 \cdot 10^{-2}, & \text{if } x \in (200,400], \\ -2.8341 \cdot 10^{-10} \cdot x^3 + 9.6359 \cdot 10^{-7} \cdot x^2 - 4.1144 \cdot 10^{-4} \cdot x + 6.9707 \cdot 10^{-2}, & \text{if } x \in (400,600], \\ 6.5796 \cdot 10^{-10} \cdot x^3 - 7.3089 \cdot 10^{-7} \cdot x^2 + 6.0525 \cdot 10^{-4} \cdot x - 1.3363 \cdot 10^{-1}, & \text{if } x \in (600,800], \\ 2.1852 \cdot 10^{-9} \cdot x^3 - 4.3961 \cdot 10^{-6} \cdot x^2 + 3.5375 \cdot 10^{-3} \cdot x - 9.1555 \cdot 10^{-1}, & \text{if } x \in (800,1000], \\ 3.8850 \cdot 10^{-9} \cdot x^3 - 9.4957 \cdot 10^{-6} \cdot x^2 + 8.6371 \cdot 10^{-3} \cdot x - 2.6154, & \text{if } x \in (1000,1200], \\ -4.2159 \cdot 10^{-8} \cdot x^3 + 1.5626 \cdot 10^{-4} \cdot x^2 - 1.9027 \cdot 10^{-1} \cdot x + 7.6948 \cdot 10^{1}, & \text{if } x \in (1200,\mathrm{MeT}], \\ 3.8356 \cdot 10^{-8} \cdot x^3 - 1.7538 \cdot 10^{-4} \cdot x^2 + 2.6507 \cdot 10^{-1} \cdot x - 1.3145 \cdot 10^{2}, & \text{if } x \in (\mathrm{MeT},\mathrm{CMeT}], \\ 1.1633 \cdot 10^{-8} \cdot x^3 - 4.2857 \cdot 10^{-5} \cdot x^2 + 4.6012 \cdot 10^{-2} \cdot x - 1.0746 \cdot 10^{1}, & \text{if } x \in (\mathrm{CMeT},1760], \\ -1.5470 \cdot 10^{-7} \cdot x^3 + 8.3536 \cdot 10^{-4} \cdot x^2 - 1.4996 \cdot x + 8.9604 \cdot 10^{2}, & \text{if } x \in (1760,1800]. \end{cases}$$

Electrical conductivity (S/m)

Previous research (England et al. 1968) suggested that the electrical conductivity of solid lunar regolith is close to zero. However, other researchers (Olhoeft et al. 1974) found that lunar regolith displays an exponentially-temperature dependent electrical conductivity while it is heated, which means that the value of electrical conductivity of molten lunar regolith is likely to be higher than zero. Thus, they formulated equations for highlands (temperature between 573.15 K to 1,500 K) and mare (temperature between 298.15 K to 873.15 K) regolith, respectively. Because these models do not share the same temperature region, Schreiner et al. (2016) suggested a single model with a Vogel-Tamman-Fulcher (VTF) equation as below

$$\sigma_e = e_a \exp\left(\frac{-e_b}{T-T_g}\right)$$

where $\boldsymbol{\sigma_e}$ is electrical conductivity (S/m), *T* is the temperature (K), T_g is the glass transition temperature, and e_a and e_b are regression coefficients. It was noted that T_g should be set to zero to avoid vertical asymptotes in the low-temperature regime. Initially, Schreiner et al.'s approach did not work well in COMSOL due to (i) the extreme thermal discontinuity between the boundaries of the air and the specimen domains, and (ii) too high precision of the *EC* value (over e^{-22} to e^{-89} which exceeds the COMSOL's precision of e^{-16}). Through some experiments, it was found that *1 + EC – α* where *α* value is close to one would be an ideal formula for eliminating the high precision issue; thus, we have adjusted the equation as $1 + \sigma_e\text{-}9.99999999999999e^{-1}$ (see Figure 5).

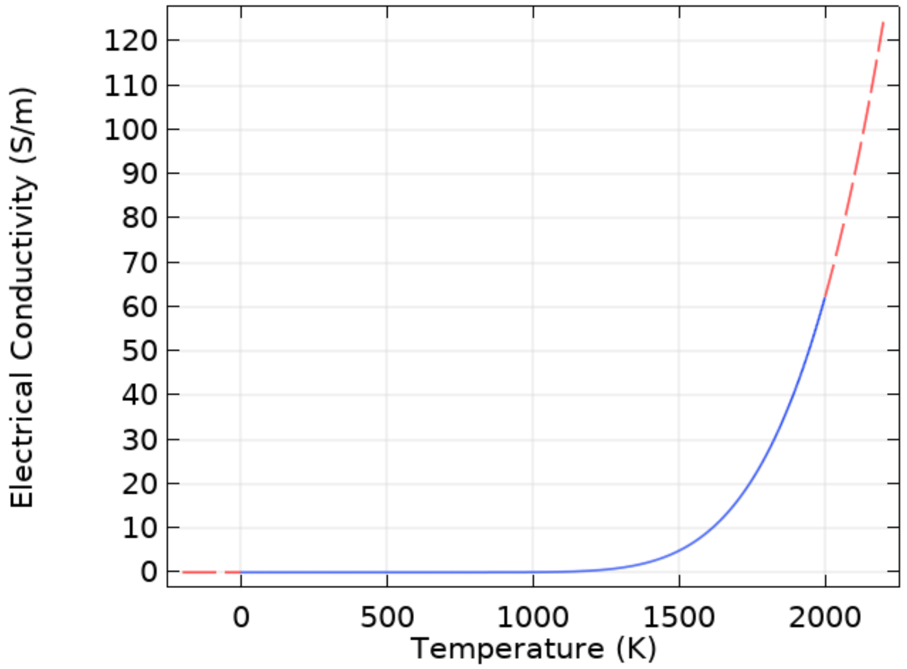

Figure 5: Material properties – Electrical Conductivity of highlands regolith as a function of temperature with a $1 + \sigma_e\text{-}9.99999999999999e^{-1}$ formula.

Relative permittivity (ε'– iε") and Relative permeability (μ' – iμ")

Permittivity and the loss tangent (tanδ) are the most important material properties in microwave processing. The relative (or complex) permittivity indicates the ability of a dielectric to absorb and store electrical energy, with the real permittivity (*ε'*) (also known as the dielectric constant) and the imaginary permittivity, dielectric loss factor (*ε"*). *S*imilarly, the relative permeability is compounded by permeability constant (*μ'*) and imaginary permeability, magnetic loss factor (*μ"*). On the other hand, the loss tangent indicates the ability of the material to convert absorbed energy into heat (National_Research_Council 1994). Although the dielectric constant can vary with frequency and temperature, the existing works (Barmatz et al. 2011, Ethridge and Kaukler 2012) measured both the relative permittivity and relative permeability of lunar regolith/simulant as a constant value rather than a function of temperature (e.g. Barmatz et al. (2011) measured both values from multiple frequencies, in which the deviation of the values is reasonably minimal; thus we have used a mean value of Barmatz et al.'s work for this experiment (see Table 1).

Table 1: Mean values of the relative permittivity and relative permeability of lunar regolith where ε′ is Dielectric Constant, ε″ is dielectric loss factor, μ′ is Permeability Constant and μ″ is magnetic loss factor. (estimated from (Barmatz et al. 2011)).

Relative Permittivity				Relative Permeability			
Highlands		Mare		Highlands		Mare	
ε′	ε″	ε′	ε″	μ′	μ″	μ′	μ″
3.14531	0.01038	3.62544	0.041565	1.09474	0.00175	0.99949	0.003655

3.3 Other settings for the simulation of the microwave heating model in COMSOL

- Input frequency and power: The input frequency is set at 2.45 GHz, which is the same as in domestic microwaves we tested before. For this simulation, we have used seven input powers – 50 W, 100 W, 200 W, 400 W, 600 W, 800 W and 1,000 W.
- Study setting: For the simulation, a pre-defined Microwave Heating Multiphysics with a 'Frequency-Transient' study have been used. The input port is set as a coaxial port following the bespoke microwave configuration.
- Specimen size: Three specimen size are prepared for this experiment – Large (2.5 x 3.45 cm cylinder), medium (2 x 3 cm cylinder), and small (0.72 x 1.2 cm cylinder) specimens (Figure 6). The temperature of the specimen was measured as a volume (blue object in Figure 7a) and 12 sampled points (red dots in Figure 7b). As we set the density at 2.07 g/cm^3, the mass of each specimen is 35 g, 19.5 g and 1 g, respectively.

- Specimen support: The specimen sits on the base support (an alumina ceramic plate), which is almost transparent to microwave energy similar to quartz glass installed in the top and bottom of the cavity. The support is also included in the microwave heating simulation, and it contributes a conductive heat transfer with the specimen only (Figure 8).
- Microwave heat configuration: In this experiment, two different heat configurations have been used. The first configuration includes conductive heat transfer only in order to mimic an airless cavity environment with a radiant barrier that can be applied for designing a 3D printer on the Moon. Omitting the air domain for the simulation of a heat transfer physics also helps for reducing the convergence errors during simulation caused by the extreme thermal discontinuity between the air and the surface of the specimen. The second configuration includes conductive and radiative heat transfer to compare the heat performance of both configurations.
- The boundary condition of the cavity: In our model, the skin depth of the cavity is much smaller than the model dimensions at the given frequency, which means that the electromagnetic (EM) fields and currents will penetrate only a very short distance into the cavity material (in our case, aluminium). In this case, the Electromagnetic Wave (EMW) Physics in COMSOL does not need to be active in the domain of cavity skin; thus, we have deactivated the EMW inside the metal domain. Besides, it is usually efficient to model the metal as a surface but not a volume due to the computational benefit.
- Hotspot: The bespoke microwave includes two tuning methods. One is the industrial standard three stub tuners, which maximises microwave input power, and the other is the vertical cylindrical tuner, which is used to minimise the reflected power and to adjust the location of the hotspot. The hotspot of the cavity is vertically aligned with the centre of the cavity (see Figure 7c); thus, a specimen is placed in a central position

accordingly. In this experiment, the position of the vertical tuner is optimised and fixed for the medium-size specimen to provide the same condition to each specimen size.

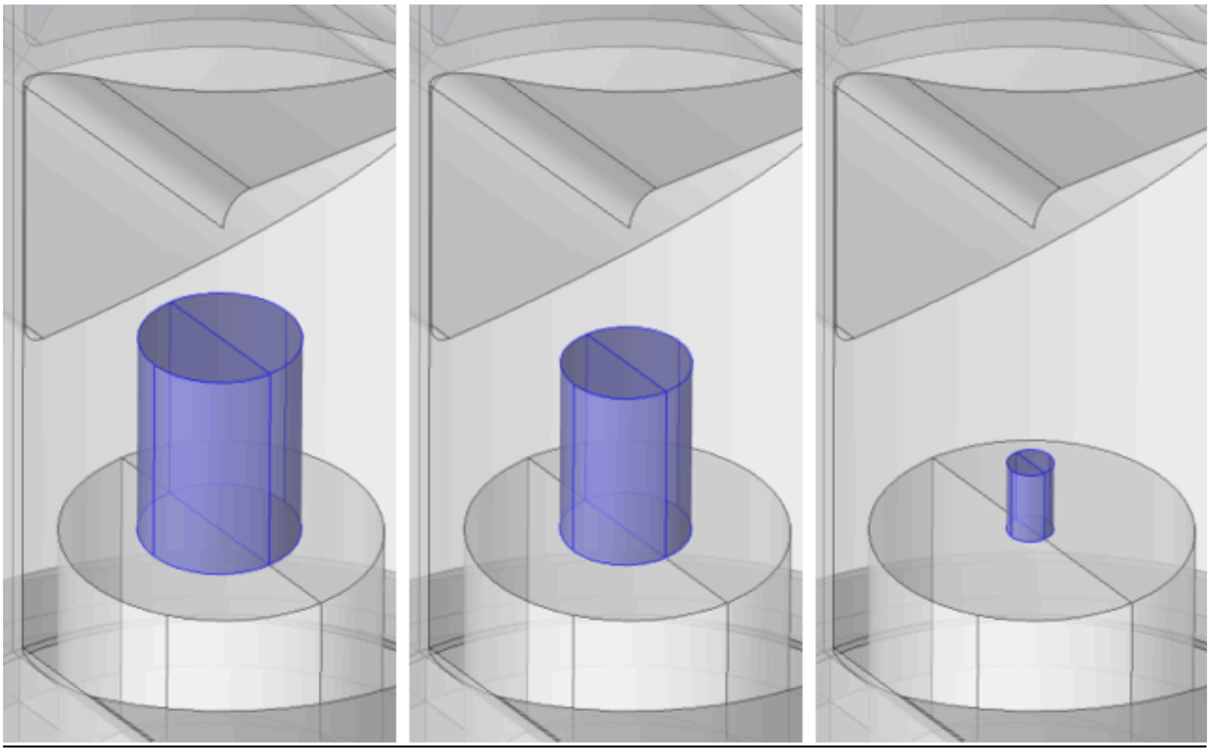

(a) (b) (c)

Figure 6: Three specimen sizes (diameter x height). (a) Large – 2.5 x 3.45 cm, (b) medium - 2 x 3 cm, (c) small - 0.72 x 1.2 cm.

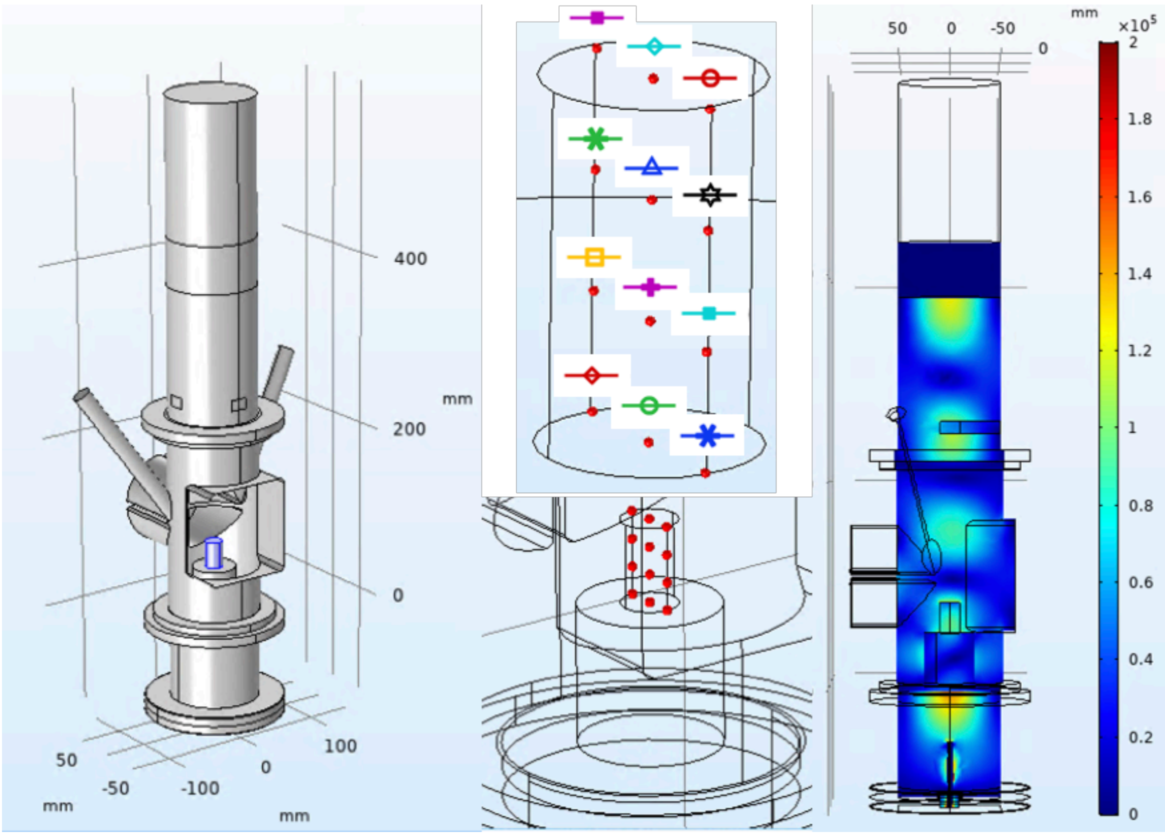

(a) (b) (c)

Figure 7: Barebones of the bespoke microwave cavity in COMSOL. (a): The cavity with a medium specimen, (b): 12 sampled points (red dots) in the medium specimen with the legend of temperature plots in this paper, (c): Electric field in the cavity with a medium specimen of highlands regolith.

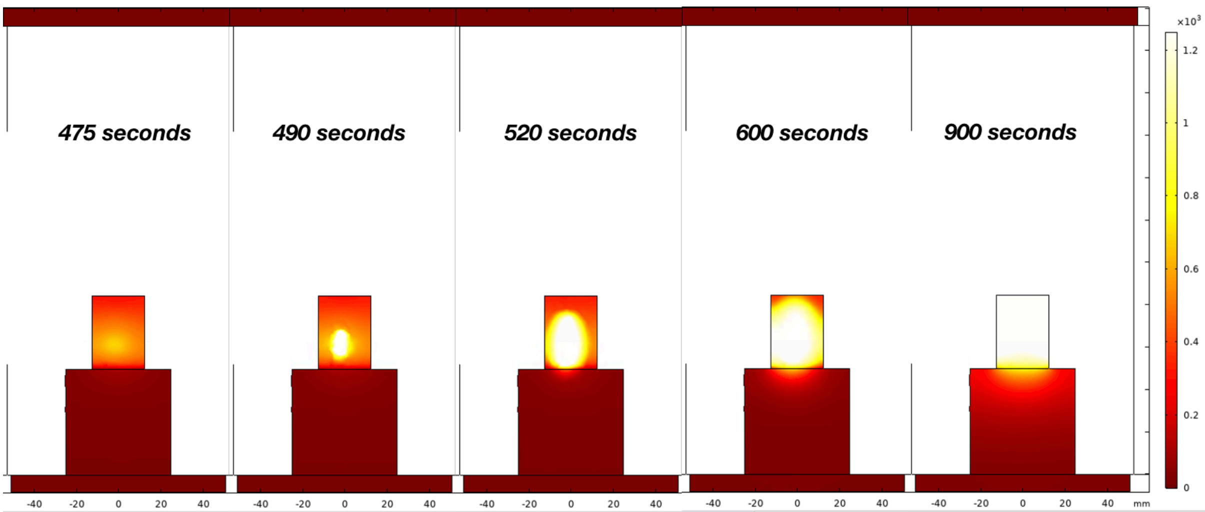

Figure 8: Snapshot of the microwave heating simulation of a medium specimen of highlands regolith under 1,000 W of input power for different heating times.

Because an understanding of the microwave heating process of new material is still empirical and speculative to some degree due to its highly nonlinear character (Vriezinga et al. 2002) with variables including material properties, the shape, dimension and position of a specimen in a cavity, most research in microwave processing of material is exploratory (National_Research_Council 1994). Moreover, in the case of lunar regolith we are trying to understand an extra-terrestrial material which may not be fully understood yet with respect to the laws of physics; thus, we have adopted an empirical approach in this work. For example, to determine the above settings, a total of 190 sets of simulations were conducted. The work presented in this paper used a total of 75 sets – new 63 sets (21 sets for each size) of the simulation without radiative heat transfer and new 12 sets of simulation with radiative heat transfer.

4. Comparison of the simulation outputs

Following our previous lab-experiment using JSC-1A, we prepared three specimen sizes, large (35 g) which can be directly compared with our previous experiment, medium (19.5 g) and small (1 g). The reason for a 1-gram specimen is to find out whether the bespoke microwave is suited for heating (sinter/melt) such a small mass of lunar regolith/simulant as any real lunar regolith samples are likely to be made available in similar quantities. The maximum and minimum temperature of each specimen with seven input powers in 100 and 900 seconds are summarised in Table 2 for large specimens, Table 3 for medium specimens and Table 4 for small specimens.

4.1 Large specimen (2.5 x 3.45 cm cylinder with 35 g mass)

Firstly, we have simulated a large specimen with seven input powers (50 W, 100 W, 200 W, 400 W, 600 W, 800 W, 1,000 W).

Table 2: Comparison of microwave heating simulation of large specimens. The values represent the maximum and minimum temperature in the specimen of each category in 100 and 900 seconds respectively.

Input Power (W)	Highlands (Max & Min temperature °C)		Mare High-Ti (Max & Min temperature °C)		Mare Low-Ti (Max & Min temperature °C)	
	100 s	900 s	100 s	900 s	100s	900 s
1,000	260.87 34.50	1508.20 548.06	379.33 45.51	1482.70 569.20	375.23 45.30	1481.4 568.49
800	235.75 32.07	1373.60 390.74	332.12 40.97	1399.00 492.49	328.84 40.82	1395.00 490.55
600	210.03 29.65	700.63 72.64	286.50 36.45	1277.70 390.30	283.96 36.33	1276.00 388.69
400	177.35 27.13	444.03 53.58	239.08 31.82	1106.30 265.66	237.19 31.74	1100.60 263.15
200	134.19 24.17	308.93 37.63	179.19 26.86	484.57 53.08	177.83 26.82	475.25 52.70
100	101.50 22.40	224.91 29.82	135.36 24.03	310.16 37.21	135.18 24.03	308.22 37.10
50	79.64 21.45	165.78 25.63	102.30 22.35	225.51 29.61	101.53 22.34	224.09 29.55

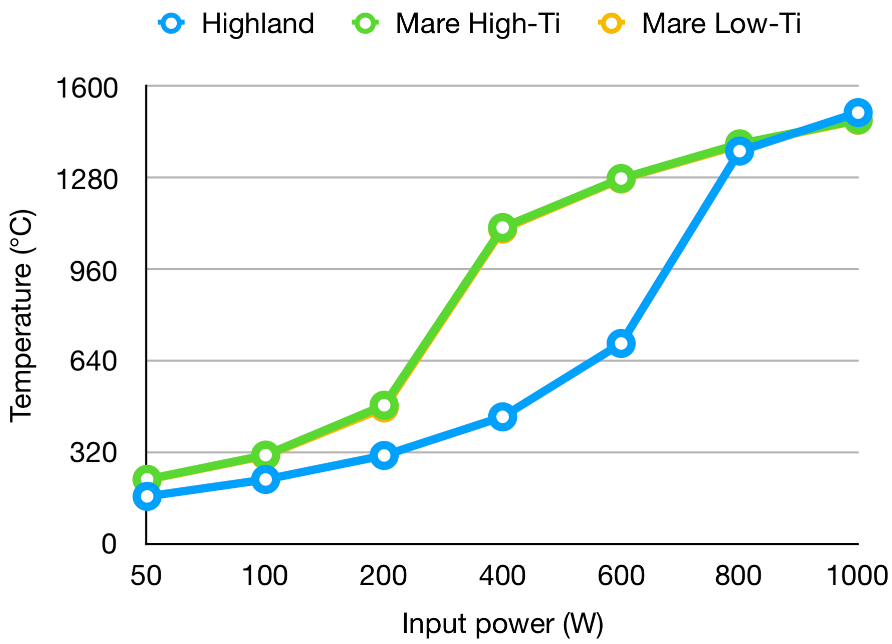

Figure 9: The heating trend of large specimen of each material through the seven input powers with 900 seconds of heating time. Note that mare High-Ti and mare Low-Ti regolith display an almost identical trend.

The heating trend of each material through the seven input powers clearly shows that mare regoliths have very different behaviour compared to highlands regolith regarding microwave energy absorption. The following observations are made:

- *The heating trend by input power*: The heating rates of both highlands and mare specimen are relatively low until 200 W, after which mare specimens display rapid increases between 200 and 400 W, while highlands specimen displays a similar rapid increase between 600 and 800 W (Figure 9). As the material properties of this numerical model address neither the particle size distribution nor irregular shape, the main reason for the difference could be the amount of FeO, i.e. 6.2 wt% for highlands regolith and 16.6~17.0 wt% for mare regolith.
- *Sintering/melting purpose*: Figure 9 shows that the highlands regolith couples with microwave energy less efficiently compared with the mare regolith under lower input power, i.e. less than 800 W. Although, the highlands and mare specimens did not reach the melting temperature in 900 seconds under 600 W and 200 W of input

power respectively, both specimens experience extreme temperature increase under higher input powers. The temperature curves of three specimens indicate that two sampled points of each specimen have thermal runaway effect, which may not be an ideal situation for manufacturing/construction purpose (see more discussion in Section 5), while other points are also radically heated (see Figure 10). Note that the bottom three sampled points show much lower temperature curves due to the conductive heat transfer to the support of the specimen.

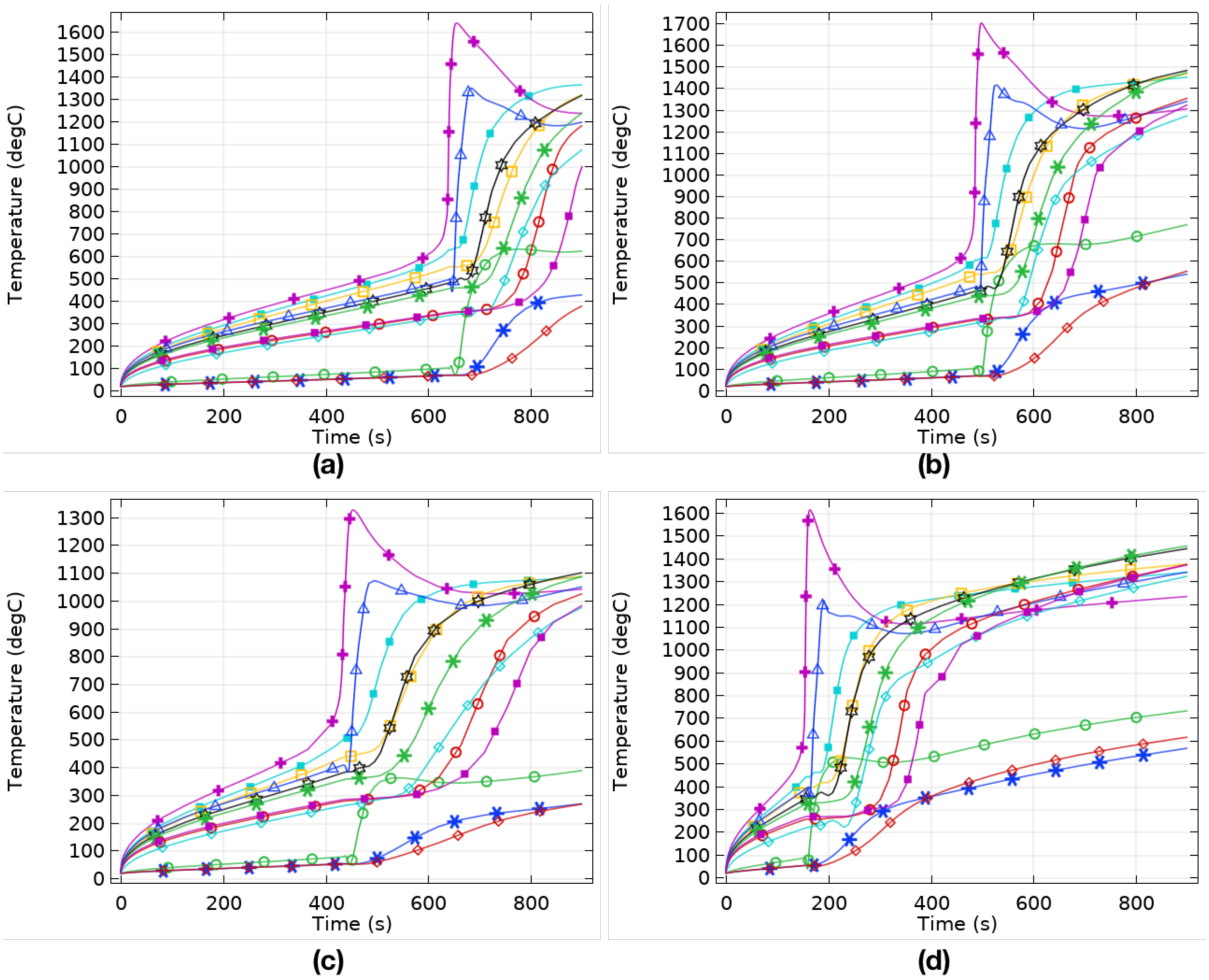

Figure 10: Temperature of the 12 sampled points in a large specimen of highlands and mare High-Ti regolith under different input power to 900 seconds. (a) Highlands 800 W, (b) Highlands 1,000 W, (c) Mare High-Ti 400 W, (d) Mare High-Ti 1,000 W. (see the legend in Figure 7b)

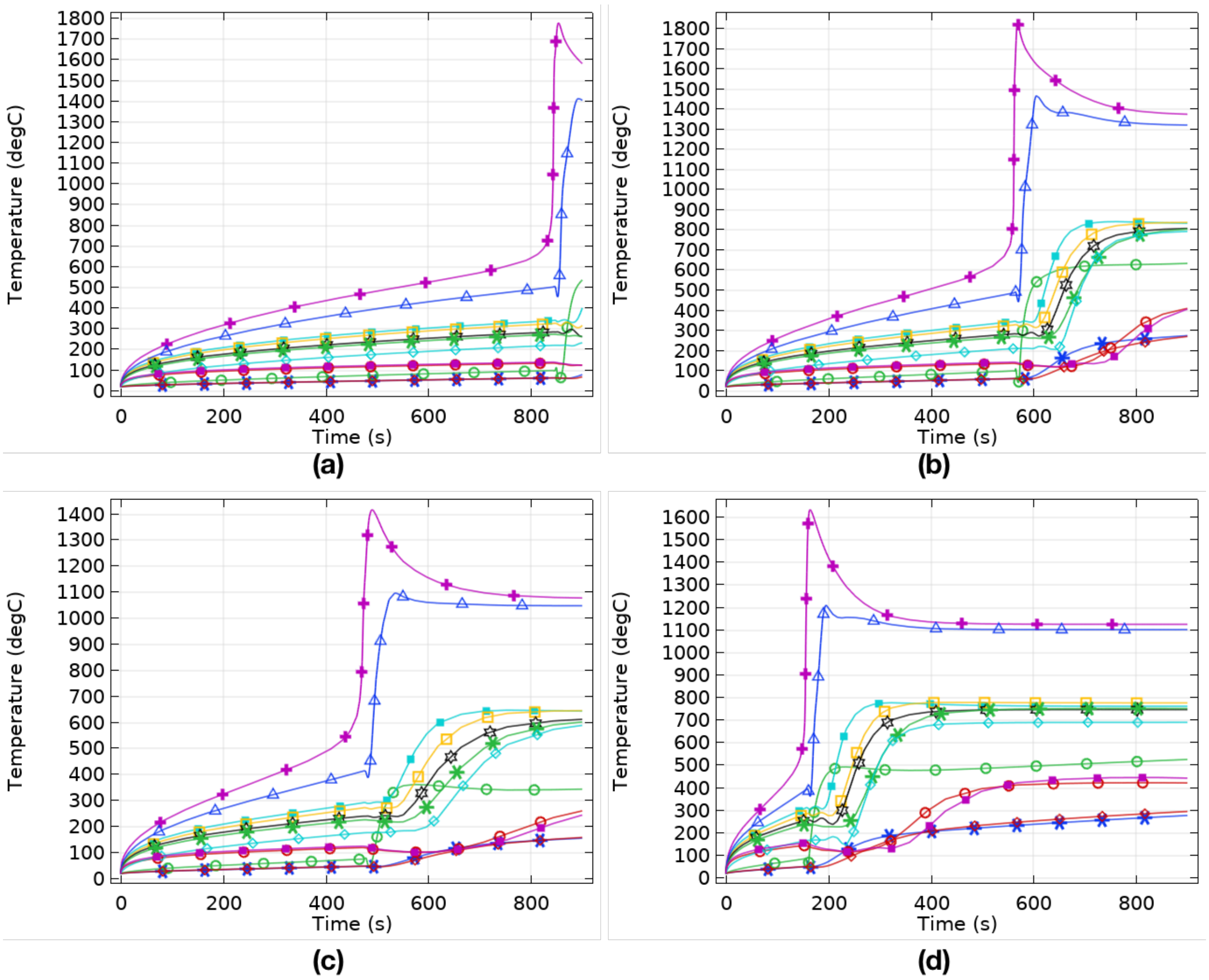

Figure 11: Temperature of the 12 sampled points in a large specimen with radiative heat transfer under different input power to 900 seconds. (a) Highlands 800 W, (b) Highlands 1,000 W, (c) Mare High-Ti 400 W, (d) Mare High-Ti 1,000 W. (see the legend in Figure 7b)

Despite the higher convergence errors of the simulation with radiative heat transfer, all large-sized specimens were successfully simulated (Figure 11). Apart from the two sample points experiencing thermal runaway (the temperature curves of pink-cross and blue-triangle marks), the temperature of the rest of the sample points was lower and stabilised due to the temperature loss through radiative heat transfer. The highlands specimen had thermal runaway with a higher temperature than the one without radiative heat transfer, while the mare High-Ti specimen was almost the same. For both highlands specimen (Figure 11a and Figure 11b), thermal runaway occurred later than the one without radiative heat transfer

(Figure 10a and Figure 10b) due to the slow incremental rise in temperature, which did not happen to the mare High-Ti specimen.

4.2 Medium specimen (2 x 3 cm cylinder with 19.5 g mass)

Following the settings of the large specimen, we have also simulated a medium specimen with seven input powers (50 W, 100 W, 200 W, 400 W, 600 W, 800 W, 1,000 W).

Table 3: Comparison of microwave heating simulation of medium specimens. The values represent the maximum and minimum temperature in the specimen of each category in 100 and 900 seconds respectively.

Input Power (W)	Highland (Max & Min temperature °C)		Mare High-Ti (Max & Min temperature °C)		Mare Low-Ti (Max & Min temperature °C)	
	100 s	900 s	100 s	900 s	100 s	900 s
1,000	441.65 56.08	1855.60 876.47	1280.50 310.73	1772.70 770.50	1286.30 306.35	1766.90 768.67
800	385.32 49.27	1784.40 800.01	1305.50 239.82	1691.80 708.93	1311.80 235.61	1689.40 708.33
600	329.29 42.68	1676.40 685.37	1376.00 126.85	1598.50 630.46	1385.80 121.71	1611.40 633.83
400	271.22 36.19	1504.90 508.37	1557.50 59.99	1472.10 515.50	1573.30 59.67	1465.10 513.72
200	201.45 29.33	544.93 62.48	350.15 44.02	1239.70 331.11	346.60 43.82	1237.20 330.25
100	152.11 25.46	355.91 40.73	249.47 33.97	1040.40 202.73	247.51 33.43	1037.60 201.81
50	115.49	255.01	186.09	611.93	184.71	564.97

	23.20	31.22	27.83	54.35	27.78	53.94

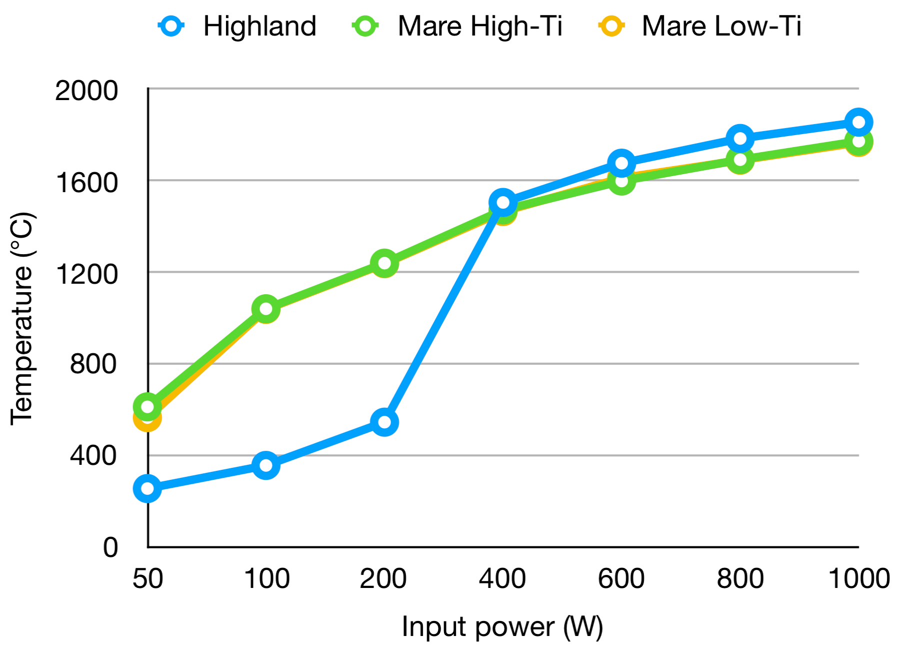

Figure 12: The heating trend of medium-sized specimen of each material through the seven input powers with 900 seconds of heating time. Note that the trends for mare High-Ti and mare Low-Ti regolith are almost identical.

The heating trend of the medium-sized specimen contrasts sharply with the large specimen under lower input power, and the output indicates some interesting things as below:

- *The heating trend by input power*: Both highlands and mare specimens show high-temperature increment, while the highlands specimen shows a radical increase between 200 W and 400 W of input power and then follows the heating trend of the mare specimens with slightly higher temperature as shown in Figure 12. The temperature curves of highlands specimen are similar to the large specimen of highlands regolith although thermal runaway occurs much faster by the input power.
- *Sintering/melting purpose*: Despite the smaller mass and volume, the medium specimens are better coupled with microwave energy than the large specimens. All three regoliths experience extreme thermal runaway more quickly with a slightly

higher temperature than the large specimens; consequently, reaching far beyond the complete molten temperature (1,653K, 1,379.85 °C). Unlike the large specimen, even the highlands specimen is also mostly melted in 650 seconds under 400 W of input power while the mare specimens are mostly melted in 900 seconds under 200 W (see Figure 13). Note that the bottom three sampled points are also heated to a higher temperature than the large specimens.

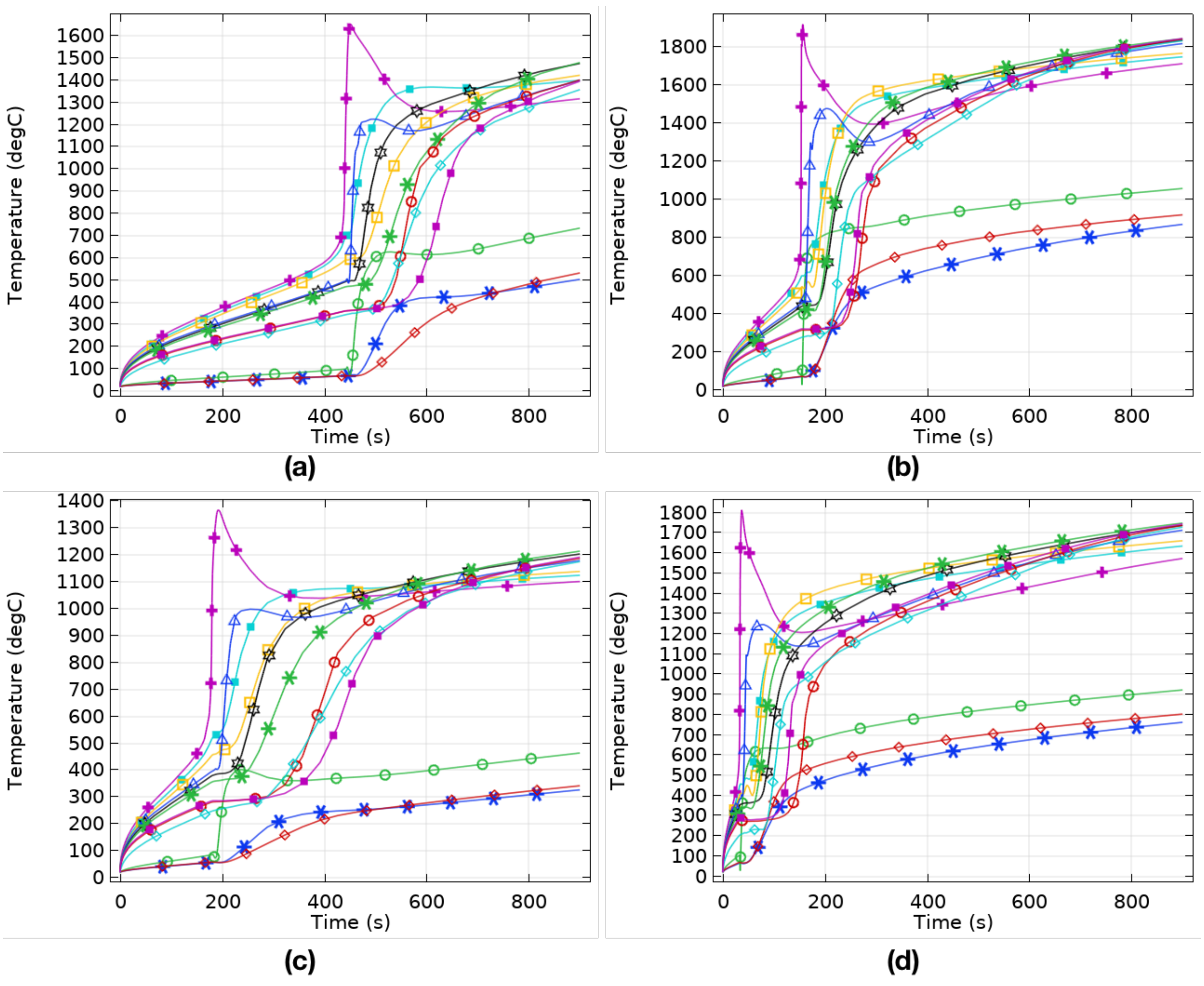

Figure 13: Temperature of the 12 sampled points in a medium-sized specimen of highlands and mare High-Ti regolith under different input power to 900 seconds. (a) Highlands 400 W, (b) Highlands 1,000 W, (c) Mare High-Ti 200 W, (d) Mare High-Ti 1,000 W. (see the legend in Figure 7b)

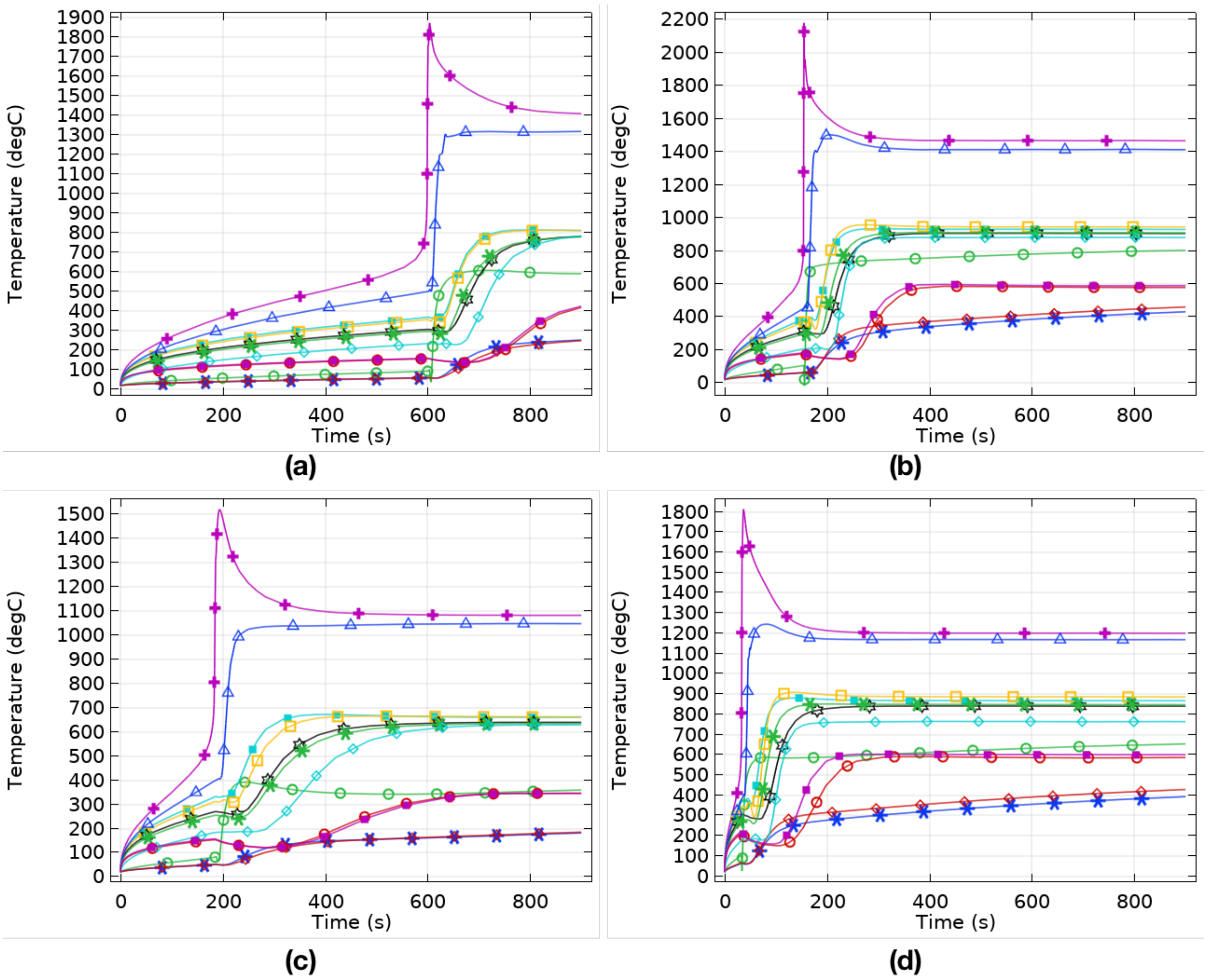

Figure 14: Temperature of the 12 sampled points in a medium specimen with radiative heat transfer under different input power to 900 seconds. (a) Highlands 400 W, (b) Highlands 1,000 W, (c) Mare High-Ti 200 W, (d) Mare High-Ti 1,000 W. (see the legend in Figure 7b)

The medium-size specimens with radiative heat transfer (Figure 14) show similar patterns with the large-size specimens. Apart from the two sample points facing thermal runaway (the temperature curves of pink-cross and blue-triangle marks), the temperature of the rest of the sample points was lower and stabilised due to the temperature loss through radiative heat transfer. Besides, the highlands specimen had thermal runaway with a much higher temperature than the one without radiative heat transfer, while the mare High-Ti specimen was almost the same. For the highlands specimen under 400 W input power (Figure 14a), thermal runaway occurred later than the one without radiative heat transfer (Figure 13a) due to the slow increment of the temperature, which did not happen to the other three specimens.

4.3 Small specimen (0.72 x 1.2 cm cylinder with 1 g mass)

As mentioned earlier, we also have simulated heating of 1 gram of lunar regolith to check if the bespoke microwave equipment can be used with such a small mass/volume of materials.

Table 4: Comparison of microwave heating simulation of small specimens. The values represent the maximum and minimum temperature in the specimen of each category in 100 and 900 seconds respectively.

Input Power (W)	Highland (Max & Min temperature °C)		Mare High-Ti (Max & Min temperature °C)		Mare Low-Ti (Max & Min temperature °C)	
	100 s	900 s	100 s	900 s	100 s	900 s
1,000	173.30 25.26	417.52 33.88	316.68 34.97	2164.70 1202.20	314.00 34.85	2164.90 1202.50
800	157.58 24.45	373.86 31.33	283.18 32.40	2104.40 1051.00	281.16 32.31	2106.60 1062.20
600	139.76 23.59	321.75 28.70	248.00 29.83	2032.40 925.54	246.14 29.76	2033.40 929.27
400	118.08 22.62	260.10 26.01	206.00 27.12	1928.40 763.71	204.50 27.07	1924.80 757.82
200	90.69 21.56	190.69 23.38	152.97 24.23	358.44 30.58	152.02 24.20	355.53 30.49
100	67.73 20.89	139.30 21.91	116.88 22.56	253.72 25.72	115.97 22.54	252.06 25.68
50	52.73	98.43	83.97	184.85	87.53	183.78

	20.52	21.07	21.49	23.20	21.48	23.19

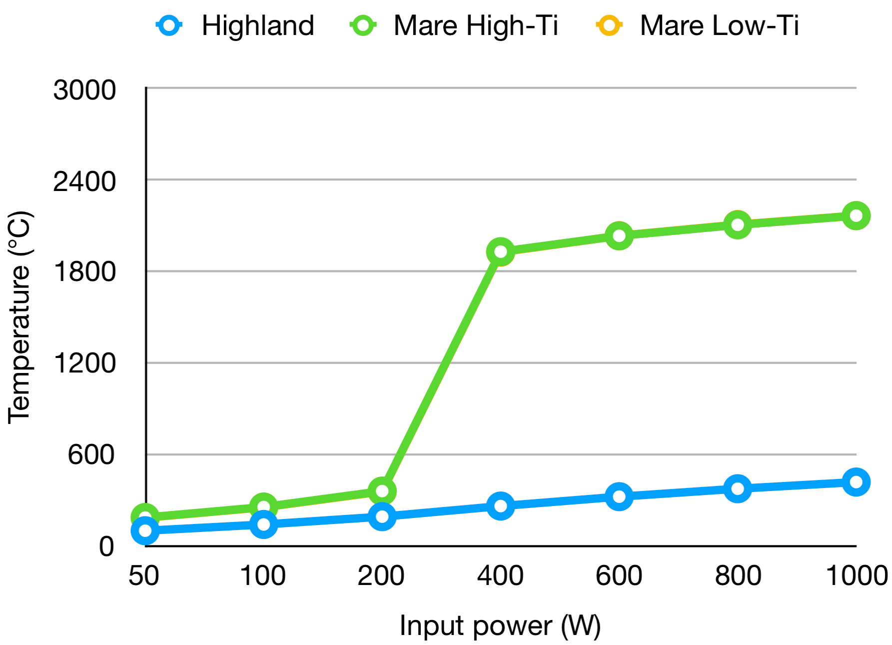

Figure 15: The heating trend of small-sized specimen of each material through the seven input powers with 900 seconds of heating time. Note that the trends for mare High-Ti and mare Low-Ti regolith are almost identical.

The heating trend of the small-sized specimen is very different from other sizes, and the output reveal the following:

- *The heating trend by input power*: Due to the conductive and radiative heat transfer from the specimen to the base, the bottom three sample points are much less heated than other points. The temperature of the highlands specimen reached less than 450 °C in 900 seconds under 1,000 W of input power, while the mare specimens were heated surprisingly well and reached a much higher temperature than of the medium specimens (see Table 4 and Figure 15). The heating rates of both mare specimens are rapidly increased between 200 and 400 W, while the highlands specimen is mildly increased.

- *Sintering/melting purpose*: The temperature curves of the highlands (1,000 W, Figure 16a) and mare High-Ti specimens (200 W, Figure 16b) are interestingly similar. Besides, the thermal runaway effect of the mare specimens is extraordinary. As shown in Figure 16c and Figure 16d, the temperatures of most sampled points were increased almost 1,000 °C less than 30 seconds. This means that small volume/mass of the mare regoliths can be instantly melted when it passes a certain threshold of input power and heating time.

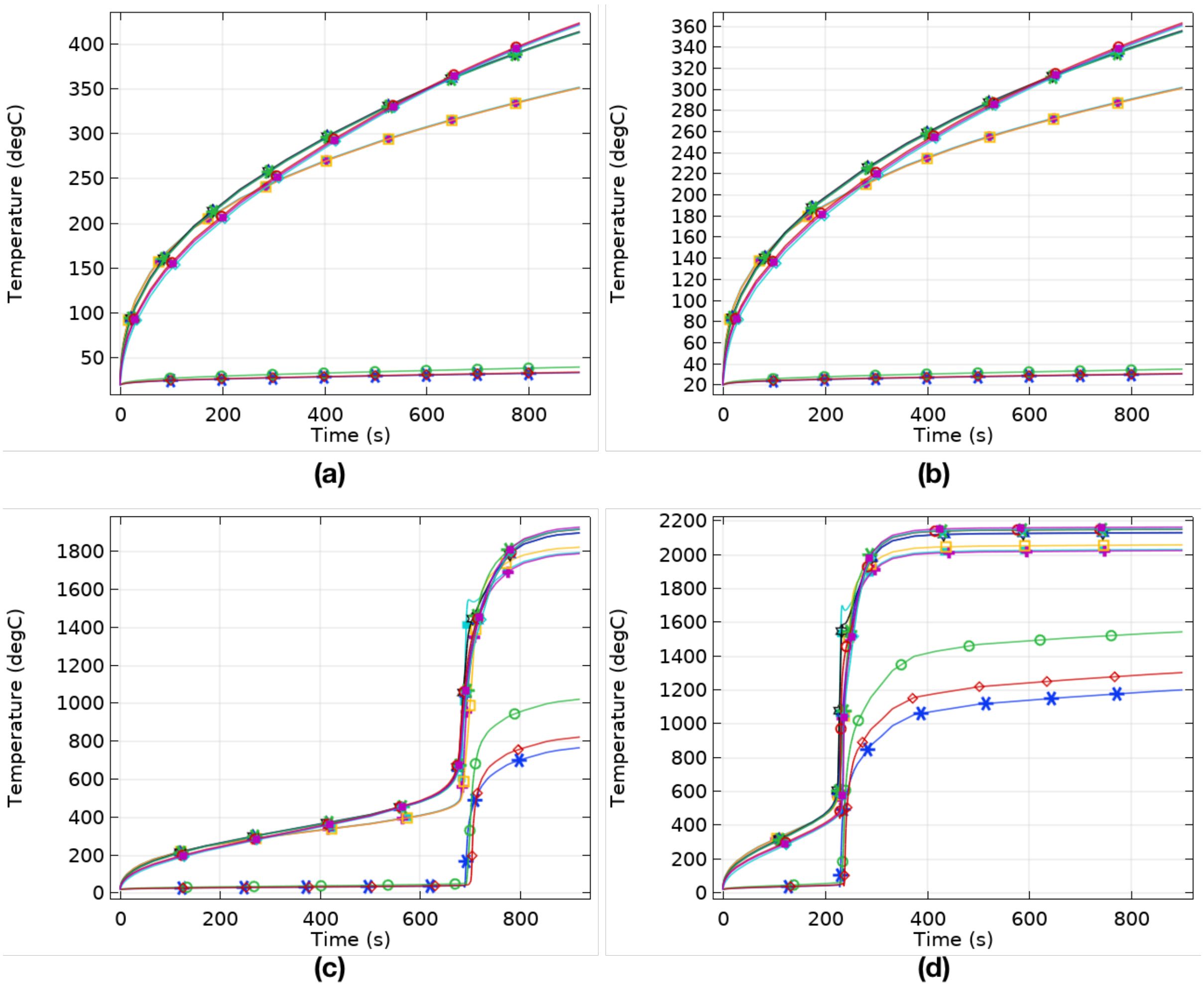

Figure 16: Temperature of the 12 sampled points in a small specimen of highlands and mare High-Ti regolith under different input power to 900 seconds. (a) Highlands 1,000 W, (b) Mare High-Ti 200 W, (c) Mare High-Ti 400 W, (c) Mare High-Ti 1,000 W. (see the legend in Figure 7b)

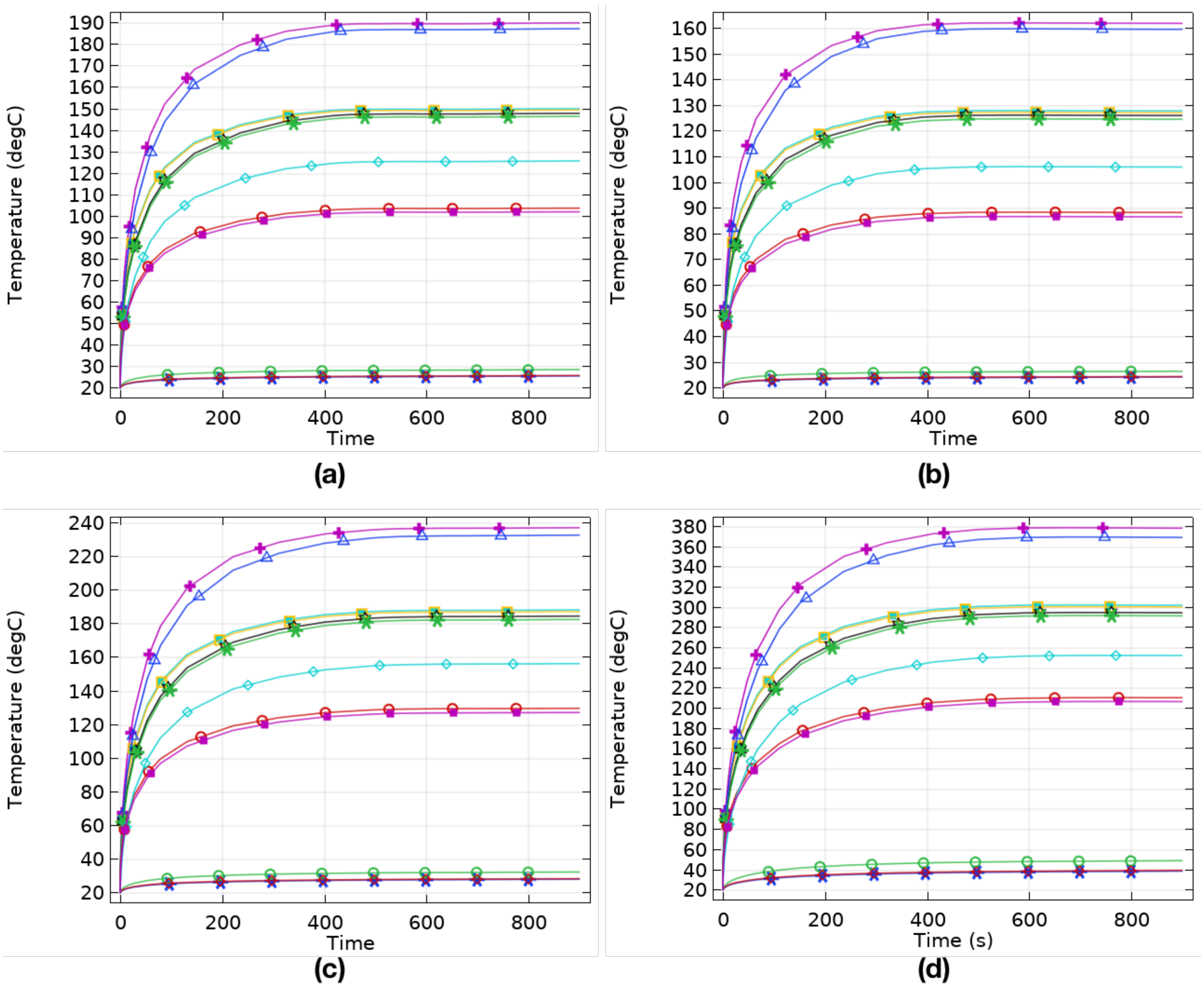

Figure 17: Temperature of the 12 sampled points in a small specimen with radiative heat transfer under different input power to 900 seconds. (a) Highlands 1,000 W, (b) Mare High-Ti 200 W, (c) Mare High-Ti 400 W, (d) Mare High-Ti 1,000 W. (see the legend in Figure 7b)

In the case of small-size specimens, the effect of radiative heat loss is non-trivial. The temperature curves of the small-size specimens with radiative heat transfer barely reached 400 °C even under 1,000 W input power due to the small volume (Figure 17). Thus, the hotspot was not able to reach the threshold of thermal runaway (around 600 °C) at all; consequently, no thermal runaway was observed.

<u>5. Analysis of the simulation outputs</u>

5.1 Microwave energy absorption by the specimen volume

It is well known that microwaves can penetrate the material and supply energy resulting in generating volumetric heating (Wang et al. 2015); thus a small volume of material tends to absorb less microwave energy than a larger one. However, the simulation in this experiment shows slightly different results. The medium specimen of mare High-Ti regolith has much higher electric field than the large specimen (see Figure 18) and has more than five times higher resistive losses, which transmit electrical energy and convert it to heat, compared with a large specimen (see Table 5); consequently, the medium specimen was heated to a much higher temperature. Note that the highlands and mare low-Ti specimens also have a similar output. This could be explained as the medium specimen might have an optimal dimension and volume of the specimen with respect to the penetration depth, which plays a vital role in an efficient heating process (Sun et al. 2016), within the current cavity setting.

Table 5: Maximum electric field and resistive losses of the mare high-Ti specimens under 1,000 W of input power.

	Large specimen (2.5 x 3.45 cm cylinder, 35 g)	Medium specimen (2 x 3 cm cylinder,19.5 g)	Small specimen (0.72 x 1.2 cm cylinder,1 g)
Electric Fields (V/m)	4.183e4	9.466e4	4.574e4
Resistive Losses (W/m^3)	4.957e6	2.538e7	5.926e6

On the other hand, the small specimens of both mare regoliths show almost instant thermal runaway and much higher temperature than the large and medium specimens. Besides, their electric fields and resistive losses are also higher than the large specimen (see Table 5 and Figure 18). Thus, more research on the correlation between the cavity design and the dimension/volume/mass of specimen is needed for achieving an optimal heating performance.

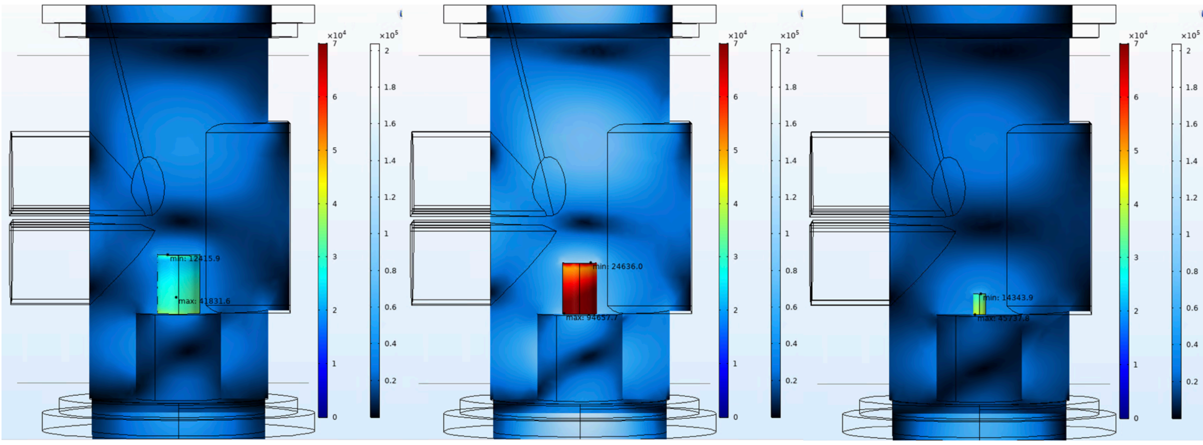

(a) (b) (c)

Figure 18: Electric field of the cavity and specimen in X-axis plane under 1,000 W with mare High-Ti specimen. (a) large, (b) medium and (c) small specimen. Note that the rainbow colour legend is for the specimen while the other is for the cavity.

5.2 Temperature increment by the regolith location

Many researchers believe that iron (FeO) in lunar regolith/simulant would be one of the primary reasons for better microwave energy absorption. Thus, some researchers even suggested to consider a hybrid heating system, which combines the sources of both microwave and conventional heat, e.g. using higher dielectric loss susceptors, insulator or coatings to more readily absorb the incident power (National_Research_Council 1994). The simulation results in this work seem to confirm that the researchers' assumption was valid in case of small specimen. The highlands regolith was barely heated while the mare regoliths were heated up quickly with thermal runaway. For the large and medium-size specimens, however, it is a completely different story. Although both mare regoliths couple with microwave energy very well and heated up much faster than highlands regolith in the early stages of heating, the highlands regolith was also heated up to temperatures as high as the mare regoliths in 900 seconds and the temperature of thermal runaway was higher than that of the mare regoliths. The convergence errors of the simulation when thermal runaway occurs are high for all three regoliths and specimen sizes, which means that the temperature of the thermal runaway may not be necessarily accurate; however, the trend of thermal runaway would be still valid. All three regoliths and three sizes (except the small specimen of highlands regolith) showed much faster heating under much less power than melting JSC-1A.

5.3 Temperature increment and thermal runaway

The results of this experiment indicate that higher input power tends to boost the speed of the early heating process in a less uniform heating manner, which results in only some parts being heated up rapidly and experience thermal runaway. Some researchers (Roussy et al. 1987, Tian et al. 1992) predicted that materials could be heated stably without thermal runaway up to specific power levels, and the result of our experiments also indicate that the lunar regoliths do not experience thermal runaway under low input power, but when it occurs, it happens quicker with higher input power.

Thermal runaway – a nonlinear phenomenon where a little increase in input power causes a significant temperature increase – is one of the most critical issues in material processing with temperature dependent dielectric properties (Santos et al. 2010), which can be explained with nonlinear feedback between microwave absorption and heat dissipation in general. However, thermal runaway only occurs when (i) the material properties are a function of temperature, and (ii) the input power is greater than a threshold (Liu and Sheen 2008). Most of the thermal runaway in this experiment starts around 600 °C, and we hypothesise that the threshold of thermal runaway (around 600 °C) might be related to the glass transition phase of the lunar regolith because the glassy phase of the material could boost electronic coupling. Our early experiment also showed that the dielectric constant of JSC-1A was noticeably increased between 600 ~ 900 °C, and this could support the above hypothesis. Besides, Liu and Sheen (2008) emphasised that the input power threshold of thermal runaway is sensitive to the geometric parameters under certain conditions. In our lab-based experiment using JSC-1A, a specimen rarely had a melted core if the height of the specimen was much shorter than the width of the specimen. As the ratio of the height to the width of the specimen in this experiment is much larger, Liu and Sheen's claim seems valid.

6. Conclusion and future work

In this work, we have formulated an experimental, numerical model of microwave heating behaviour of three lunar regoliths from the existing works and simulated the model with seven input powers and three volumes/masses of a specimen.

Although the input power and heating time required for each regolith to be sintered/melted vary depending on the size of the specimen and regolith, microwave heating of lunar regolith seems plausible, in general, because lunar regolith couples exceptionally well with microwave energy. For highlands regolith, it may require additional processing, e.g., a hybrid heating system, which combines the sources of both microwave and conventional heating, e.g. using higher dielectric loss susceptors, insulator or coatings to more readily absorb the energy if the input power is low and the dimensions of cavity and material are not optimal as shown in the simulations of 35 grams and 1 gram case. Besides, radiative heat loss seems significant; thus, an effective and efficient radiant barrier for a cavity needs to be considered for improving the heating performance. Nevertheless, the outcomes have revealed the necessity of future work as summarised below to build upon the work presented in this paper.

- *Material properties as a function of temperature*: As discussed earlier, some material properties – relative permittivity, relative permeability, heat capacity and thermal conductivity – need to be updated as a complete function of temperature to produce more valid outputs. Besides, the electrical conductivity is defined as zero due to the configuration issue discussed earlier.

- *Thermal runaway:* The results clearly show the sign of thermal runaway for all three regolith and much higher temperature increase in general. In Figure 13c and Figure 13d, which illustrate the medium-size specimens, two sample points of both mare specimens experience thermal runaway in 85 seconds under 400 W (1,600 °C), in 55 seconds under 600 W (1,700 °C), in 45 seconds in 800 W (1,750 °C) and 35 seconds in 1,000 W (1,800 °C), while other points are barely heated less than 500 °C. There seems a specific correlation between the input power, heating time and temperature to trigger thermal runaway, which can be possibly considered as a threshold. Thus, a future experiment should be planned to (i) understand the threshold of input power and geometric parameters, which causes thermal runaway, and (ii) optimise the microwave heating behaviour of lunar regolith.
- *Phase change material (PCM) simulation*: Modelling of PCM condition is crucial because this experiment simulates microwave heating behaviour of lunar regolith above the melting point for some parts of the material. This condition requires more parameters, including a latent heat value of melting for lunar regolith, and it makes the model very complicated. Thus, we have not added it in this experiment for the same reasons with the radiative heating condition.
- *Design and experiment of other frequency-based cavities*: The penetration depth of microwave increases with a long wavelength (lower frequencies) while it decreases with a short wavelength (high frequencies). Thus, the microwave heating behaviour of lunar regolith would also be altered. For example, the half power penetration depth of 2.45 GHz is around 65 cm (Taylor and Meek 2005) and could fabricate a 0.96 ~ 1.2 cm sintered layer or 0.59 ~ 1.34 cm of a melted layer (Allan et al. 2013). With lower frequencies, microwave can penetrate regolith further (Ethridge and Kaukler 2012), but it would not sinter the regolith effectively. Considering lunar ISRU activities, including oxygen and water production, the lower frequency would be a

better option as it requires a longer heating process with a deeper penetration depth for industrial-scale production. On the other hand, a shallow penetration depth with higher frequency might be a better option if the heating process focuses on a surface finishing, e.g. fabricating pavement on the lunar surface. Therefore, different microwave frequencies than 2.45 GHz, e.g. 915 MHz and 5.8 GHz, need to be investigated. Note that the design/dimension of the cavity also needs to be updated to apply different frequencies.

Acknowledgement

The authors are grateful for the financial support from the Open University's Strategic Research Area (SRA) funding. The authors also thank Professor Andrew Holland and Mrs Vibha Levin Prabhu at the Open University for their early technical inputs into designing the bespoke microwave equipment, and particular thanks to Dr Martin B. Barmatz at NASA JPL for his comprehensive advice regarding the value of the permittivity and permeability of lunar regolith. The authors also highly appreciate the invaluable comments from the editor and two anonymous reviewers that helped improve the quality of this manuscript. MA acknowledges support from a UK Space Agency (UKSA) grant (# ST/R001391/1) and a STFC grant (# ST/P000665/1) that partially supported this work.

References

Allan, S., Braunstein, J., Baranova, I., Vandervoort, N., Fall, M. and Shulman, H. (2013). "Computational Modeling and Experimental Microwave Processing of JSC-1A Lunar Simulant." Journal of Aerospace Engineering Vol. 26, No. 1, pp.143-151. http://dx.doi.org/10.1061/(ASCE)AS.1943-5525.0000245.

Anand, M., Crawford, I. A., Balat-Pichelin, M., Abanades, S., van Westrenen, W., Péraudeau, G., Jaumann, R. and Seboldt, W. (2012). "A brief review of chemical and mineralogical resources on the Moon and likely initial in situ resource utilization (ISRU) applications." Planetary and Space Science Vol. 74, No. 1, pp.42-48. http://dx.doi.org/10.1016/j.pss.2012.08.012.

Barmatz, M., Steinfeld, D., Winterhalter, D., Rickman, D. and Weinstein, M. (2013). Microwave Heating Studies and Instrumentation for Processing Lunar Regolith and Simulants. 44th Lunar and Planetary Science Conference. The Woodlands, Texas, LPI

Barmatz, M. B., Steinfeld, D., Begley, S. B., Winterhalter, D. and Allen, C. (2011). Microwave permittivity and permeability measurements on lunar soils. 42nd Lunar and Planetary Science Conference, Houston, USA, Lunar and Planetary Institute.

Colozza, A. J. (1991). Analysis of Lunar Regolith Thermal Energy Storage. NASA Contractor Report 189073, Lewis Research Center Under Contract NAS3-25266

Crawford, I. (2015). "Lunar Resources: A Review." Progress in Physical Geography Vol. 39, No. pp.137-167. https://dx.doi.org/10.1177/0309133314567585.

Cremers, C. J. (2012). "Thermophysical properties of Apollo 14 fines." Journal of Geophysical Research Vol. 80, No. 32, pp.4466-4470. 10.1029/JB080i032p04466.

England, A. W., Simmons, G. and Strangway, D. (1968). "Electrical conductivity of the Moon." Journal of Geophysical Research Vol. 73, No. 10, pp.3219-3226. 10.1029/JB073i010p03219.

Ethridge, E. and Kaukler, W. (2012). Finite Element Analysis of Three Methods for Microwave Heating of Planetary Surfaces. 50th AIAA Aerospace Sciences Meeting including the New Horizons Forum and Aerospace Exposition, American Institute of Aeronautics and Astronautics. pp.AIAA2012-0801. https://doi.org/10.2514/6.2012-801.

Ethridge, E. and Kaukler, W. (2012). Microwave Extraction of Volatiles for Mars Science and ISRU. Concepts and Approaches for Mars Exploration. Houston, TX

Ethridge, E. C. and Kaukler, W. (2011). Microwave Processing of Planetary Surfaces for the Extraction of Volatiles. 49th AIAA Aerospace Sciences Meeting including the New

Horizons Forum and Aerospace Exposition, Orlando, Florida, 4-7 January, AIAA. http://dx.doi.org/10.2514/6.2011-612.

Hayne, P. O., Bandfield, J. L., Siegler, M. A., Vasavada, A. R., Ghent, R. R., Williams, J. P., Greenhagen, B. T., Aharonson, O., Elder, C. M., Lucey, P. G. and Paige, D. A. (2017). "Global Regolith Thermophysical Properties of the Moon From the Diviner Lunar Radiometer Experiment." Journal of Geophysical Research: Planets Vol. 122, No. 12, pp.2371-2400. http://dx.doi.org/10.1002/2017JE005387.

Heiken, G. H., Vaniman, D. T., French, B. M. and Schmitt, H. H. (1991). Lunar Sourcebook - A user's guide to the Moon. Cambridge, UK, Cambridge University Press.

Hemingway, B. S., Robie, R. A. and Wilson, W. H. (1973). Specific heats of lunar soils, basalt, and breccias from the Apollo 14, 15, and 16 landing sites, between 90 and 350°K. Proceedings of the Lunar Science Conference, Vol 4, p2481.

Hoogenboom, R., Wilms, T. F. A., Erdmenger, T. and Schubert, U. S. (2009). "Microwave-Assisted Chemistry: a Closer Look at Heating Efficiency." Australian Journal of Chemistry Vol. 62, No. 3, pp.236-243.

Kang, Y. and Morita, K. (2006). "Thermal Conductivity of the CaO-Al2O3-SiO2 System." ISIJ International Vol. 46, No. 3, pp.420-426. 10.2355/isijinternational.46.420.

Langseth, M. G., Clark, S. P., Chute, J. L., Keihm, S. J. and Wechsler, A. E. (1972). "The Apollo 15 lunar heat-flow measurement." The moon Vol. 4, No. 3, pp.390-410. 10.1007/BF00562006.

Levin Prabhu, V., Lim, S., Bowen, J., Cowley, A., Katrib, J., Dodds, C. and Anand, M. (2018). Microwave heating of lunar simulants JSC-1A and NU-LHT-3M: Experimental and theoretical analysis. European Lunar Symposium (ELS2018), Toulouse, France, 13-16 May, ELS.

Lim, S., Levin Prabhu, V., Anand, M. and Taylor, L. (2017). "Extra-terrestrial construction processes - advancements, opportunities and challenges." Advances in Space Research Vol. 60, No. 7, pp.1413-1429. https://doi.org/10.1016/j.asr.2017.06.038 Corrigendum: https://doi.org/10.1016/j.asr.2018.03.022.

Liu, C. and Sheen, D. (2008). "Analysis and control of the thermal runaway of ceramic slab under microwave heating." Science in China Series E: Technological Sciences Vol. 51, No. 12, pp.2233-2241. 10.1007/s11431-008-0221-7.

Marcus, G. L., Jr., Stephen, J. K. and John, L. C., Jr. (1973). Chapter. 9: Heat Flow Experiment. Apollo 17 Preliminary Science Report, NASA SP-330, NASA

McKay, D. S., Heiken, G., Basu, A., Blanford, G., Simon, S., Reedy, R., French, B. M. and Papike, J. (1991). The lunar regolith - Chapter 7. Lunar sourcebook - A User's Guild to the Moon. G. H. Heiken, D. T. Vaniman, B. M. French and H. H. Schmitt. Cambridge, UK, Cambridge Univerisity Press. pp.285-356.

Mitchell, J. K., Houston, W. N., Carrier, W. D. I. and Costes, N. C. (1974). "Apollo soil mechanics experiment S-200, Final report, NASA Contract NAS 9–11266." Space Sciences Laboratory Series Vol. 15, No. 7.

Murase, T. and McBirney, A. R. (1970). "Thermal Conductivity of Lunar and Terrestrial Igneous Rocks in Their Melting Range." Science Vol. 170, No. pp.165-116.

National_Research_Council (1994). Microwave Processing of Materials. Washington, DC, The National Academies Press. 10.17226/2266.

Olhoeft, G. R., Frisillo, A. L., Strangway, D. W. and Sharpe, H. (1974). "Temperature dependence of electrical conductivity and lunar temperatures." The moon Vol. 9, No. 1, pp.79-87. 10.1007/BF00565394.

Reiss, P. (2018). "A combined model of heat and mass transfer for the in situ extraction of volatile water from lunar regolith." Icarus Vol. 306, No. pp.1-15. https://doi.org/10.1016/j.icarus.2018.01.020.

Roussy, G., Bennani, A. and Thiebaut, J. (1987). "Temperature Runaway of Microwave Irradiated Materials." Journal of Applied Physics Vol. 62, No. 4, pp.1167—1170.

Santos, T., Costa, L., Valente, M. A., Monteiro, J. and Sousa, J. (2010). 3D Electromagnetic Field Simulation in Microwave Ovens: a Tool to Control Thermal Runaway. Proceedings of COMSOL Conference, Paris, France.

Schreiner, S. S., Dominguez, J. A., Sibille, L. and Hoffman, J. A. (2016). "Thermophysical property models for lunar regolith." Advances in Space Research Vol. 57, No. 5, pp.1209-1222. https://doi.org/10.1016/j.asr.2015.12.035.

Stebbins, J. F., Carmichael, I. S. E. and Moret, L. K. (1984). "Heat capacities and entropies of silicate liquids and glasses." Contributions to Mineralogy and Petrology Vol. 86, No. 2, pp.131-148. 10.1007/BF00381840.

Sun, J., Wang, W. and Yue, Q. (2016). "Review on Microwave-Matter Interaction Fundamentals and Efficient Microwave-Associated Heating Strategies." Materials (Basel, Switzerland) Vol. 9, No. 4, pp.231. 10.3390/ma9040231.

Taylor, L., Hill, E. and Liu, Y. (2005). Unique lunar soil properties for ISRU microwave processing. Space Resources Roundtable VII: Lunar Exploration Analysis Group Conf. on Lunar Exploration. Houston, Lunar and Planetary Institute

Taylor, L. A. and Liu, Y. (2010). Important considerations for lunar soil simulants. Earth and Space 2010: Engineering, Science, Construction, and Operations in Challenging Environments, Honolulu, Hawaii, American Society of Civil Engineers (ASCE). http://dx.doi.org/10.1061/41096(366)14.

Taylor, L. A. and Meek, T. T. (2004). Microwave Processing of Lunar Soil. Proceedings of International Lunar Conference 2003 / International Lunar Exploration Workshop Group 5, American Astronautical Society.

Taylor, L. A. and Meek, T. T. (2005). "Microwave sintering of lunar soil: properties, theory, and practice." Journal of Aerospace Engineering Vol. 18, No. 3, pp.188-196. http://dx.doi.org/10.1061/(ASCE)0893-1321(2005)18:3(188).

Tian, Y. L., Feng, J. H., Sun, L. C. and Tu, C. J. (1992). Computer Modeling of Two Dimensional Temperature Distributions in Microwave Heated Ceramics. Materials Research Society Symposium Proceedings, Pittsburgh, Pennsylvania, Materials Research Society.

Vriezinga, C. A., Sánchez-Pedreño, S. and Grasman, J. (2002). "Thermal runaway in microwave heating: a mathematical analysis." Applied Mathematical Modelling Vol. 26, No. 11, pp.1029-1038. https://doi.org/10.1016/S0307-904X(02)00058-6.

Wang, W., Zhao, C., Sun, J., Wang, X., Zhao, X., Mao, Y., Li, X. and Song, Z. (2015). "Quantitative measurement of energy utilization efficiency and study of influence factors in typical microwave heating process." Energy Vol. 87, No. pp.678-685. https://doi.org/10.1016/j.energy.2015.05.036.